ELSEVIER

Surface Science 405 (1998) 87–103

surface science

# UHV simulation of the electrochemical double layer: adsorption of $HClO_4/H_2O$ on Au(111)

G. Pirug *, H.P. Bonzel

*Institut für Grenzflächenforschung und Vakuumphysik, Forschungszentrum Jülich, D-52425 Jülich, Germany*

Received 11 September 1997; accepted for publication 20 December 1997

**Abstract**

The coadsorption of $HClO_4$ and $H_2O$ on Au(111) has been studied as a model system of the electrolyte–interface interaction under UHV conditions by means of HREELS, LEED, XPS and AES. Exposure of Au(111) surfaces to nearly anhydrous $HClO_4$ results in molecular adsorption at sufficiently low temperatures ($\sim$130 K). As expected from the $C_s$ symmetry of the $HClO_4$ molecule, eight intramolecular A′ modes are observed by vibrational spectroscopy using HREELS. Long range order has been observed by LEED in the monolayer regime ($\Theta = 0.28$), where a $(\sqrt{3} \times \sqrt{3})R30^\circ$ structure occurred. Molecular $HClO_4$ gradually desorbs upon annealing to higher temperature, leaving perchlorate ($ClO_4$) behind, either directly adsorbed or interacting with residual $H_2O$ on the surface. These two species give rise to different ($ClO_3$) stretching vibrations at 1210 $cm^{-1}$ and 1145 $cm^{-1}$, the latter resembling the vibrational spectrum of solvated $ClO_4^-$ anions in solution. While these "solvated" species desorb beyond 203 K, directly adsorbed perchlorate is stable up to at least 273 K.

The coadsorption of $H_2O$ induces the dissociation of molecularly adsorbed $HClO_4$ partly "solvated" or directly adsorbed. The ratio of "solvated" and directly adsorbed $ClO_4$ species depends on the molecular stoichiometry between $H_2O$ and $ClO_4$. An anneal of a coadsorbed $H_2O/HClO_4$ layer to 190 K results in the formation of a $\begin{pmatrix} 3 & 1 \\ -1 & 2 \end{pmatrix}$ pattern, with mostly oxonium perchlorate ($H_3O^+ClO_4^-$) present on the surface as deduced from the observed vibrational modes. 

*Keywords:* Chemisorption; Electron energy loss spectroscopy (EELS); Gold; Low energy electron diffraction (LEED); Water; X-ray photoelectron spectroscopy; $HClO_4$; $H_3O^+ClO_4^-$

## 1. Introduction

The interaction of electrolyte consisting of mobile conducting ions and solvent with an electrode plays an important role in electrochemistry. Different approaches exist to investigate the chemical processes at this liquid/solid interface [1]. Traditionally, capacitance measurements or cyclic voltammetry have been conducted to study the adsorption/desorption behavior of the constituents of the electrolyte as a function of the applied potential [2]. On the basis of these "in situ" experiments, models have been developed in order to describe the structural, chemical and electronic situation in the electrochemical double layer which determine the properties of electrochemical cells. More recently, surface sensitive methods became available which allow the characterisation of such liquid/solid interfaces more directly [3–8]. While optical methods such as X-ray scattering [9], infrared reflection absorption spectroscopy (IRAS) [10], second harmonic generation (SHG) [11] or sum-frequency generation (SFG) [12], as well as

* Corresponding author. Fax: (+49) 2461 613907; e-mail: g.pirug@fz-juelich.de

0039-6028/98/$19.00 
PII: S0039-6028(98)00055-7

imaging probes like scanning electron tunneling or atomic force microscopy (STM [13] and AFM [14]) can be applied under real "in situ" conditions, electron spectroscopies require special UHV environments. Emersion "ex situ" techniques have been developed to transfer the samples with intact double layer into the UHV systems [15,16]. The study of coadsorbed electrolyte components on electrode materials represents a further attempt to come to a more detailed understanding of the situation in the inner Helmholtz layer, next to the electrode surface [3]. In contrast to "in situ" or "ex situ" experiments this "non situ" surface science approach allows the characterisation of the chemical interaction between the electrolyte ions, the solvent and the electrode surface decoupled from the influence of the external potential applied in electrochemical cells [7].

This study is an example of the "non situ" type experiment dealing with the adsorption of molecular hydrogen perchlorate $HClO_4$ and its interaction with coadsorbed water on Au(111) surfaces. In a foregoing paper we tried to characterise this system by photoelectron spectroscopy [17]. The main results were that $HClO_4$ and $H_2O$ do not mix under sequential adsorption but stay separated in different layers at sufficiently low temperature of about 80 K. Intermixing occurs upon heating to higher temperatures, leading to the formation of hydrated perchlorate complexes. The thermal stability of these species decreases with increasing amount of hydration water, as deduced from the desorption temperature, which ranges between 210 K for anhydrous perchloric acid and 150 K for fully hydrated perchlorate. The maximum hydration number has been estimated to be about 7 [17]. Under the given experimental conditions it was not possible to determine the chemical nature of the various adsorbed species from the measured O 1s and Cl 2p photoemission peaks. Obviously the chemical shift between these species was too small for a separation into different contributions for the chosen energy resolution of the hemispherical photoelectron analyser. No structural information could be gained in that system. Therefore we reinvestigated the adsorption of perchloric acid on Au(111) by vibrational spectroscopy (HREELS) combined with LEED and AES to get a more detailed picture. For coverage calibration and easier comparison with the preceding study we applied photoelectron spectroscopy (XPS) supplemented by LEED and AES in a second UHV chamber.

## 2. Experimental

Both UHV systems used for this investigation operate at a base pressure lower than $5 \times 10^{-11}$ mbar and are equipped with a quadrupole mass spectrometer (QMS) for residual gas analysis, a LEED optics for surface structure determination and a cylindrical mirror analyser for Auger electron spectroscopy (AES).

One of these systems [18] contains in addition a high resolution electron energy loss spectrometer (HREELS) for vibrational spectroscopy, while the coverage calibration and surface composition have been determined in the second UHV chamber [19] equipped also with XPS.

Since this paper is mostly based on vibrational data, the HREEL spectrometer should be described in more detail. It consists of a double stage monochromator and a single analyser. All spectra were measured in the specular direction at an incident angle of 60°. The energy resolution amounts typically to about 50–60 $cm^{-1}$ at a primary electron energy of 5–6 eV. The elastically reflected beam has usually such a high intensity that the channeltron saturates yielding no longer the right peak shape. Consequently, the elastically reflected peak is not shown in the spectra. Instead, only its position is indicated, to which all peak positions are referred with an accuracy of 5 $cm^{-1}$, according to the step width of the digitally recorded spectra. Signal averaging was achieved by adding three to five spectra, each of which is measured within about 15 min for a 4000 $cm^{-1}$ range.

The Au(111) crystals oriented with an accuracy of $\pm 0.15°$ have been mechanically polished prior to the insertion into the UHV system. Sputtering with an Ar ion beam of 5 μA and 500 eV energy for several hours followed by an anneal up to 1170 K results in a clean surface as controlled by AES. The surface crystallography was good enough to build up the $22 \times \sqrt{3}$ surface reconstruction, as observed by LEED, which is expected for

a clean Au(111) surface [20]. The sample temperature measured by a Ni/CrNi thermocouple clamped to one edge of the crystal could be varied between 1200 K and 130 K by electron bombardment and liquid nitrogen cooling, respectively.

The same specially designed dosing system has been used in both UHV systems for the $HClO_4$ exposure as shown in Fig. 1. The dosing system, which could be pumped separately by a turbomolecular pump, consists of a small glass reservoir for the liquid closed by a dosing valve, a dosing volume of well-defined size and a dosing tube, to which the front of the crystal can be faced. The pressure has been measured using a spinning rotor gauge. Compared to conventional ion gauges, there is no need for any calibration factor. Only the molecular weight of the probe gases has to be known to get absolute pressure value readings. Furthermore, the gas composition is not affected by the measurement. In principal, this dosing system allows the exposure of the sample at a constant gas flux or by emptying the fixed dosing volume. A 3:1 mixture of 96% $H_2SO_4$ and 70% $HClO_4$ has been filled in a glass bulb. The vapor pressure above this liquid, mostly containing water in the beginning, has to be pumped by a turbomolecular pump several times until a mass spectrum characteristic for $HClO_4$ is observed. The addition of $H_2SO_4$ reduces the evaporation of $H_2O$, as proposed by Stuve and co-workers [21]. The $H_2O$ partial pressure can be further suppressed by keeping the $HClO_4/H_2SO_4$ reservoir at ice water temperature. Finally, a nearly anhydrous $HClO_4$ exposure can be achieved with the right stoichiometry, as determined by O 1s and Cl 2p peak areas in the corresponding XP spectra. In order to study the influence of coadsorbed $H_2O$, the crystal could be exposed separately to $H_2O$, deionized by a Millipore station to a resistance higher than 18.2 MΩ/cm.

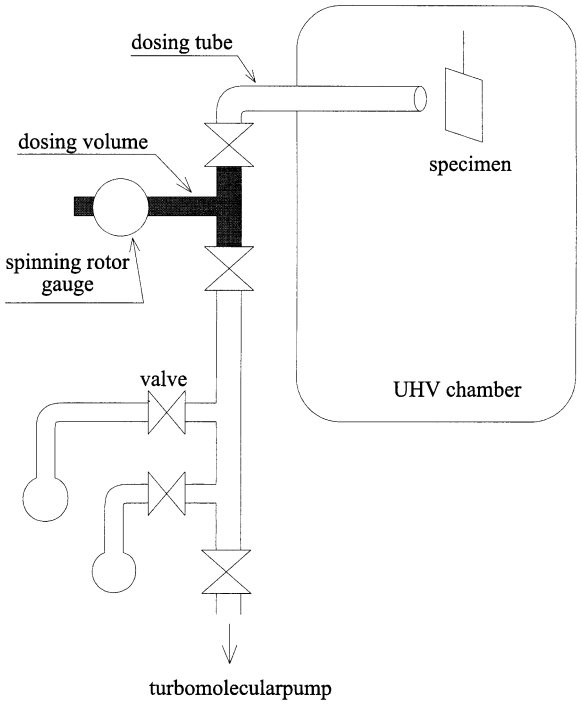


Fig. 1. Dosing system.

The coverages achieved using the dosing system can be principally determined by AES. But it turned out that the adsorbed layers are rather electron beam sensitive. This problem could be partly solved by reducing the primary current to 1 μA. Nevertheless, it was impossible to get reliable values for the $O_{KLL}$ peak intensities, neither for $HClO_4$ nor for $H_2O$, as already reported by Wieckowsky and co-workers [22,23]. Fortunately, the $Cl_{KLL}$ signal is not as sensitive to electron irradiation and could be taken as a measure for relative $HClO_4$ coverages. The AES signals were calibrated in a separate chamber equipped not only with AES but also with XPS. By comparison of the corresponding AES and XPS signals with those from well-defined potassium structures on Au(111) [24,25], absolute coverages and stoichiometries can be gained.

The Cl coverage can be calculated from the measured Cl 2p and K 2p peak areas $F$ in the XP spectra:

$$\Theta_{Cl}/\Theta_K = (\sigma^*_{K2p}/\sigma^*_{Cl2p})(F_{Cl2p}/F_{K2p}). \quad (1)$$

The atomic cross-sections $\sigma$ were taken from tabulated data [26] and corrected for the different kinetic energies $E_{kin}$ according the $1/E_{kin}$ transmission characteristic of the hemispherical analyser used (EA 10, Leybold) [27]:

$$\sigma^*_{K2p}/\sigma^*_{Cl2p} = (\sigma_{K2p}/\sigma_{Cl2p})[E_{kin}(\text{Cl 2p})/E_{kin}(\text{K 2p})] \times (\lambda_{K2p}/\lambda_{Cl2p}). \quad (2)$$

Reliable absolute values for the electron mean free path $\lambda$ are hardly available. Fortunately, we need only the ratio of the electron mean free paths $\lambda$ which can simply be expressed by their energy dependence [28] $\lambda \sim E_{kin}^{0.66}$, yielding

$$\sigma^*_{K2p}/\sigma^*_{Cl2p} = (\sigma_{K2p}/\sigma_{Cl2p})[E_{kin}(\mathrm{Cl\ 2p})/E_{kin}(\mathrm{K\ 2p})]^{0.34}. \quad (3)$$

Knowing the relationship between the K 2p peak area $F_{K2p}$ from XPS and the intensity $I_K$ of the $K_{LMM}$ Auger transition the Cl coverage can also be determined by quantitative Auger analysis:

$$\Theta_{Cl} = (S_K/S_{Cl})(I_{Cl}/I_K)\Theta_K. \quad (4)$$

The atomic sensitivity factors $S$ can be derived from a KCl spectrum, measured by PHI [29] with a cylindrical mirror analyser of the same type as used in our experiments, yielding a sensitivity ratio of $S_K/S_{Cl} = 1.53$ for the $K_{LMM}$ and the $Cl_{KLL}$ transitions. Due to the electron beam induced disproportionation, mentioned above, the O/Cl ratio cannot be determined as reliably by AES, as already reported earlier for XPS [17]. However, it could be demonstrated by comparative experiments in the XPS chamber that nearly anhydrous $HClO_4$ exposures with O/Cl ratios close to 4 can be achieved using the same dosing system as in the EELS apparatus. The exposures for the EEL spectra are given as multiples of fixed quantities. One exposure step results in a $HClO_4$ fractional coverage of about 0.05–0.1 monolayer, referred to the atomic density of $1.39 \times 10^{15}\ cm^{-2}$ of the Au(111) surface.

## 3. Results and discussion

UHV adsorption studies allow sometimes the recognition of several chemical reaction steps, which occur simultaneously under electrochemical conditions. Consequently, we studied the interaction of nearly anhydrous $HClO_4$ with the Au(111) crystal surface and its coadsorption with $H_2O$. Since already the $HClO_4$ exposure cannot be performed absolutely $H_2O$ free, the distinction between $H_2O$ and $HClO_4$ related contributions and those of their mutual influence to the EEL spectra is very important.

To our knowledge no reference data exist concerning the $H_2O$ adsorption on Au(111). The only related UHV study we are aware of shows that $H_2O$ adsorbs rather weakly on Au(111) with an adsorption energy of 10.5 kcal/mol [30]. The TPD spectra exhibit a single zero-order peak at 157 K, which does not allow any distinction between submonolayer and multilayer adsorption. Hydrogen bonding seems to be responsible for clustering into three-dimensional islands from the earliest coverage. In order to obtain vibrational data and some structural information, we investigated the adsorption of $H_2O$ on Au(111) by HREELS, LEED and XPS.

### 3.1. $H_2O$ adsorption on Au(111)

Fig. 2 shows HREEL spectra for adsorbed $H_2O$ on Au(111) at a temperature of about 120 K, physisorbed in the monolayer and condensed in the multilayer regime. An interpretation of the observed losses can be gained by comparison with gas phase data or other adsorption systems as published in a review paper by Thiel and Madey [31]. A loss at 245 $cm^{-1}$, which was identified as the frustrated O–O translation, indicates island or cluster formation of adsorbed $H_2O$ molecules even in the lowest coverage regime. Additional broad losses appear around 835 $cm^{-1}$ and 3295 $cm^{-1}$. A scissors mode which is expected for molecular $H_2O$ around 1650 $cm^{-1}$ can hardly be discerned but becomes visible with increasing amounts of $H_2O$ as shown in Fig. 2b for a condensed ice layer. Here one observes a broad O–H stretch vibration centered at 3350 $cm^{-1}$. It is worthwhile noting that the shape of the librational bands changes significantly on going from the monolayer to the condensed layer regime. A relatively intense loss from librational modes at 725 $cm^{-1}$ is responsible for the occurrence of the corresponding overtone at 1450 $cm^{-1}$. The molecular adsorption is completely reversible as shown by the simultaneous disappearance of all losses upon annealing beyond 150 K, consistent with recent findings by Kay et al. [30].

Consistent with the significant differences in the

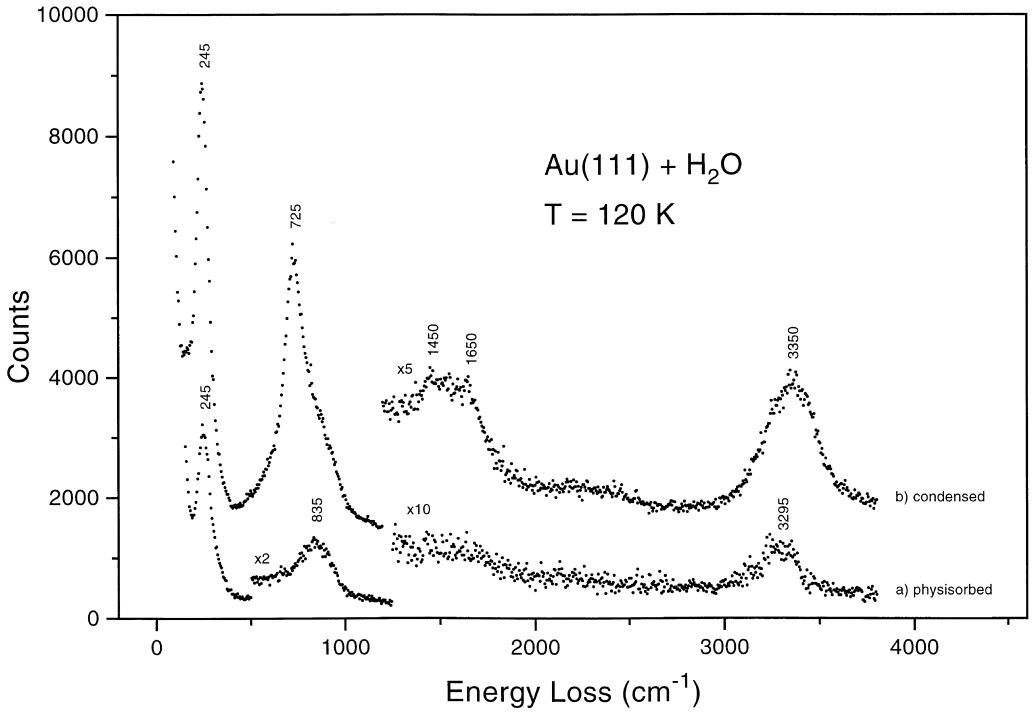


Fig. 2. HREEL spectra for $H_2O$ adsorption on Au(111) at 120 K monolayer regime, ice condensation.

vibrational loss structure, different LEED patterns have been observed, as shown in Fig. 3. In the monolayer range a $(\sqrt{3}\times\sqrt{3})R30^\circ$ structure appears without lifting the reconstruction of the underlying Au(111) surface (Fig. 3a and b). This result is in agreement with recent in situ STM measurements, which reported that the surface reconstruction of the Au(111) surface is maintained under electrochemical conditions [32]. The $(\sqrt{3}\times\sqrt{3})R30^\circ$ structure can be observed even for the lowest studied $H_2O$ coverages in support of island formation which we also deduced from the appearance of the frustrated O–O translation. This LEED pattern remains visible up to a maximum coverage of about 0.66, which is consistent with the saturation coverage of an optimal $H_2O$ bilayer [31]. A work function decrease of $\sim 0.5$ eV has been observed under these conditions. This value is relatively small compared with other transition metals such as Pt(111) [33] or Ru(001) [34], where work function changes of about 1.0 eV have been observed. Upon increasing $H_2O$ coverage the LEED pattern structure fades away into a diffuse background intensity until an incommensurate pattern structure develops for the condensed layer regime (Fig. 3c). This pattern structure is also azimuthally oriented, namely rotated by 30° with respect to the Au(111) substrate and comparable to the commensurate $(\sqrt{3}\times\sqrt{3})R30^\circ$ structure. However, the length of the reciprocal lattice vector indicates a compression by $9\pm1\%$, consistent with the difference between the lattice constant of ice of 4.52 Å [31] and the length of the unit vector of a $(\sqrt{3}\times\sqrt{3})R30^\circ$ structure on a Au(111) surface which amounts to 4.98 Å.

### 3.2. *$HClO_4$ adsorption on Au(111)*

An adsorption sequence for $HClO_4$ is shown in Fig. 4. The $HClO_4$ exposure is expressed in multiples of fixed quantities chosen as low as possible to become detectable by HREELS within reasonable measuring times. One exposure step results in fractional coverages of about 0.05–0.1 depending on the actual conditions of the dosing device. Up to about five exposure steps the

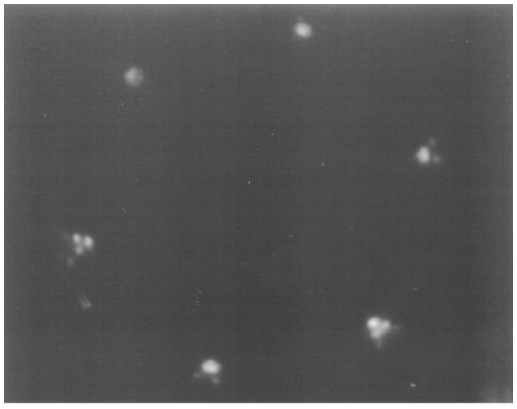

a)

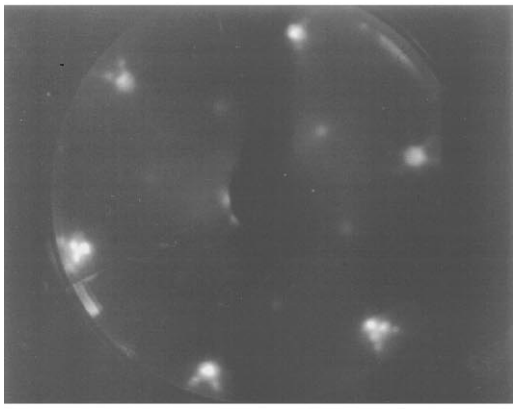

b)

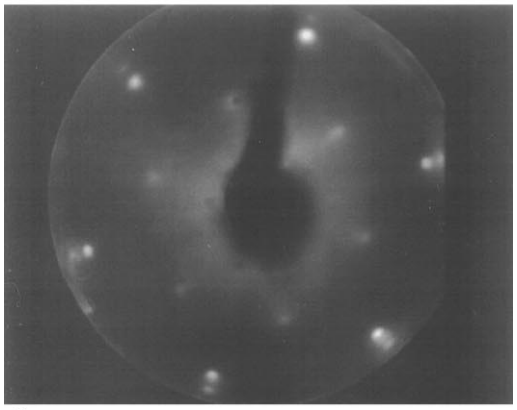

c)

Fig. 3. LEED pattern for $H_2O$ adsorbed on Au(111) at 120 K: (a) clean Au(111), $23\times\sqrt{3}$, reconstructed; (b) $H_2O$ monolayer regime, $(\sqrt{3}\times\sqrt{3})R30^\circ$; (c) ice condensation, incommensurate $(\sqrt{3}\times\sqrt{3})R30^\circ$, 9% compressed.

achieved coverage stays in the monolayer regime as suggested by the observation of a $(\sqrt{3}\times\sqrt{3})R30^\circ$ LEED pattern. The coverage of this structure has been determined by additional concomitant measurements in the XPS chamber. According to the procedures described in the experimental section, we obtained coverages of $0.27\pm0.03$ and $0.28\pm0.03$ using the XPS and AES calibration, respectively. These values approach reasonably well the coverage of 0.33 expected for an ideal $(\sqrt{3}\times\sqrt{3})R30^\circ$ structure with one adsorbed molecule per unit cell, as shown schematically in Fig. 5a. It is worthwhile noting that similar AES intensity ratios of the $Cl_{KLL}$ and $Au_{LMM}$ peaks were achieved in the XPS and HREELS chamber, as well. The anhydricity is further established by the molecular ratio determined from the O 1s and Cl 2p transition which varies between 4.01 and 4.46. Hence this $(\sqrt{3}\times\sqrt{3})R30^\circ$ structure can be considered as a result of the adsorption of hydrogen perchlorate. The spectrum obtained after 12 exposure steps corresponds to the saturation coverage for an adsorption temperature of 125 K. It turned out that failure to detect a loss at around 240 $cm^{-1}$, which has been referred to as the frustrated O–O translation of coadsorbed $H_2O$, is significant for nearly anhydrous $HClO_4$ exposure. Instead peaks at 350 $cm^{-1}$, 460 $cm^{-1}$, 590 $cm^{-1}$, 760 $cm^{-1}$, 1045 $cm^{-1}$, 1260 $cm^{-1}$ and 1330 $cm^{-1}$ are observed, which grow more or less simultaneously in intensity with increasing $HClO_4$ exposure. Apart from these major losses, less intense features can be observed at 2520 $cm^{-1}$, 2660 $cm^{-1}$, 3105 $cm^{-1}$ and 3325 $cm^{-1}$.

The adsorbed species are identified by a comparison with IR and Raman data for related compounds, applying dipole selection rules [35] to the vibrational losses shown in Fig. 4 and Fig. 6. Molecular $HClO_4$ belongs to the $C_s$ symmetry group. As such, it exhibits eight A′ and four A″ normal modes which are listed in Table 1 for gaseous, liquid and solid $HClO_4$ [36]. While all of them are IR or Raman active, only the A′ modes can be principally observed by HREEL spectroscopy [35]. $ClO_4$ fragments are also likely to occur as possible reaction products. As mentioned before, the $HClO_4$ exposure cannot be performed

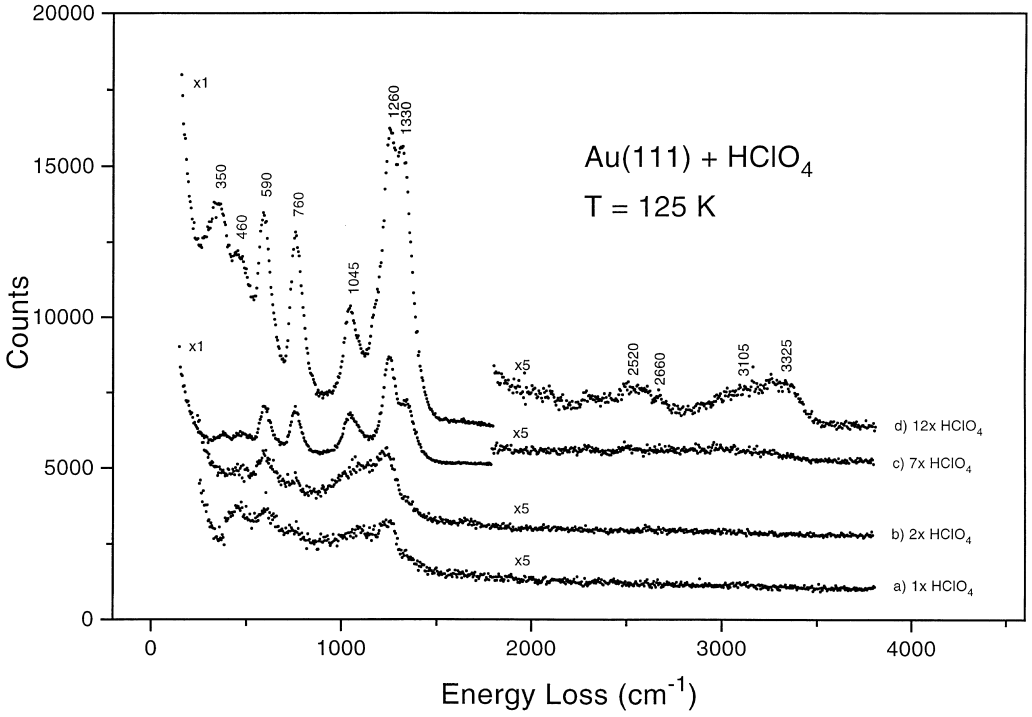


Fig. 4. HREEL spectra for $HClO_4$ adsorption on Au(111) at 125 K, doses as indicated.

completely $H_2O$ free. Hence, one has to take into account the possible interaction of coadsorbed $H_2O$ with these reaction products. In aqueous liquid electrolytes $ClO_4^-$ is considered to be a fully hydrated, non-specifically adsorbed anion. In such a configuration it belongs to the $T_d$ symmetry group with four fundamental vibrations. The corresponding IR and Raman frequencies measured in solution are included in Table 2 [37,38]. If present, the $\nu_1$ symmetric stretch frequency as the only internal $A_1$ mode should become observable by HREELS and would indicate that this complex does not interact significantly with the substrate surface. Instead, solvation by coadsorbed $H_2O$ molecules would have to be taken into account. Finally, one should consider whether unsolvated $ClO_4$ fragments are directly adsorbed analogous to specifically adsorbed anions in solution under electrochemical conditions, as observed in small quantities on Ag(110) electrodes [39]. Upon direct adsorption (chemisorption) the $T_d$ symmetry cannot be preserved due to the chemical interaction with the surface, resulting in the lifting of the degeneracy of the oxygen atoms. Oxygen atoms O* and O in contact with the substrate or pointing towards the vacuum should be distinguished. Related metal perchlorate complexes exist with the $ClO_4$ ligands in different configurations. Depending on the symmetry of either $C_{2v}$ or $C_{3v}$, four or three dipole active $A_1$ modes should be observed by HREELS, respectively. Tables 3 and 4 list normal modes of metal perchlorate complexes, as observed by IR and Raman spectroscopy. Apart from these internal vibrational modes, discussed so far, adsorbed species should vibrate as a whole against the substrate surface. But the frequency of this dipole active vibration is supposed to be very low due to the relatively large molecular weight of 100 or 99 a.u. for molecular $HClO_4$ or perchlorate $ClO_4$ species, respectively. Accordingly, these modes are difficult to be resolved and could therefore not be identified.

At first glance the HREEL spectra in Fig. 4 suggest molecular adsorption of $HClO_4$. The

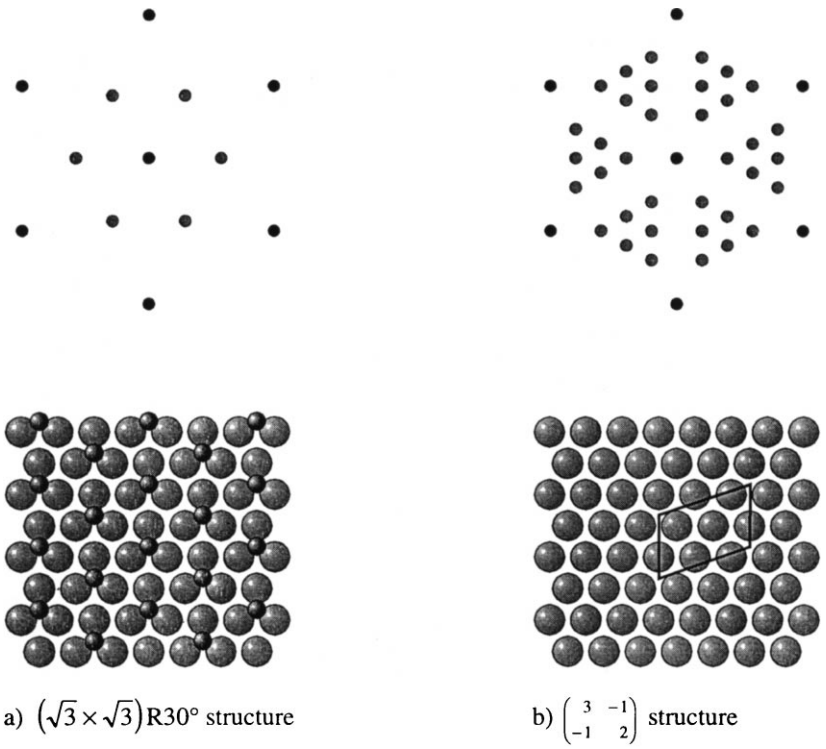


Fig. 5. Schematic LEED pattern and real space model or unit cell for (a) $(\sqrt{3}\times\sqrt{3})$R30° structure and (b) $\begin{pmatrix} 3 & -1 \\ -1 & 2 \end{pmatrix}$ structure, as observed for ($HClO_4$) and ($H_3O^+ClO_4^-$) on Au(111), respectively.

observed frequencies can be identified by comparison with tabulated infrared data for molecular $HClO_4$ (Table 1). Vibrational modes involving mainly the oxygen atoms not coordinated to H can be distinguished from those to which the OH ligand contributes significantly, denoted as $ClO_3$ and O–H modes, respectively. The occurrence of the loss at 1330 $cm^{-1}$ indicates unambiguously the presence of molecular $HClO_4$, because it can be identified as the asymmetric $ClO_3$ stretch vibration $\nu_{as}$ of molecular $HClO_4$. Consistently, the losses at 1260 $cm^{-1}$, 1045 $cm^{-1}$, 760 $cm^{-1}$, 590 $cm^{-1}$, 460 $cm^{-1}$ and 350 $cm^{-1}$ can be correlated with the O–H bending $\delta$, the symmetric $ClO_3$ stretch $\nu_s$, the symmetric Cl–OH stretch $\nu_s$, the asymmetric $ClO_3$ deformation $\delta_{as}$, the $ClO_3$ deformation $\delta_s$, and the in-plane $ClO_3$ rocking vibration $\rho$ for molecular $HClO_4$, respectively. In the O–H stretch frequency range a broad double peak around 3300 $cm^{-1}$ appears. The exact origin of the two subpeaks at 3105 $cm^{-1}$ and at 3325 $cm^{-1}$ remains unclear. By comparison with infrared frequencies for liquid and solid $HClO_4$, the contribution at 3325 $cm^{-1}$ can be assigned most likely to the O–H stretch vibration $\nu$ of molecular $HClO_4$, while the peak at 3105 $cm^{-1}$ may result from small amounts of coadsorbed hydration water. Hence all expected eight A′ dipole active modes can be observed, proving the presence of molecular $HClO_4$ with $C_s$ symmetry. Less intense peaks at 2520 $cm^{-1}$ and at 2660 $cm^{-1}$ result most likely from overtones of the strong losses at 1260 $cm^{-1}$ and 1330 $cm^{-1}$. It is worthwhile noting that substantial amounts of coadsorbed water $H_2O$ can be excluded from the absence of $H_2O$ related losses. Hence the adsorption sequence in Fig. 4 is characteristic for anhydrous molecular $HClO_4$ adsorption.

A heating sequence of a Au(111) surface saturated with $HClO_4$ at 134 K is shown in Fig. 6. Upon annealing to elevated temperatures drastic changes occur in the HREEL spectra. First of all, one observes a gradual decrease in intensity of the

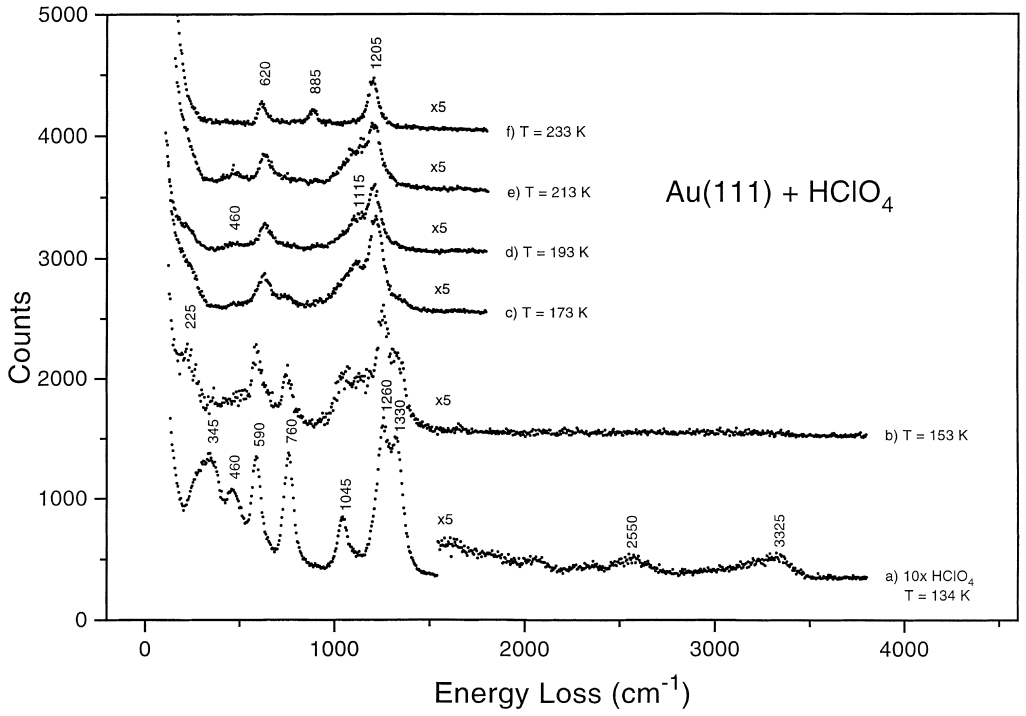


Fig. 6. HREEL spectra for $HClO_4$ adsorbed on Au(111) at 134 K and annealed to 153, 173, 193, 213 and 233 K.

Table 1
Assignment of fundamental vibrations of gaseous, liquid, solid [infrared vibrational frequencies ($cm^{-1}$)] [36] and adsorbed (this work) hydrogen perchlorate ($HClO_4$, $C_s$ symmetry)

| $HClO_4$, $C_s$ symmetry | Gaseous | Liquid | Solid | Adsorbed |
|---|---|---|---|---|
| *A′ modes* | | | | |
| $\nu$ (O–H stretch) | 3560 | 3275 | 3260 | 3325 |
| $\nu_{as}$ ($ClO_3$ stretch) | 1326 | 1315 | 1315 | 1330 |
| $\delta$ (O–H bending) | 1200 | 1245 | 1245 | 1260 |
| $\nu_s$ ($ClO_3$ stretch) | 1050 | 1041 | 1033 | 1045 |
| $\nu_s$ (Cl–OH stretch) | 725 | 743 | 760, 740 | 760 |
| $\delta_{as}$ ($ClO_3$ derformation) | 563 | 571 | 566 | 590 |
| $\delta_s$ ($ClO_3$ derformation) | 519 | ? | ? | 460 |
| $\rho$ (in-plane $ClO_3$ rocking) | 403 | ? | 371, 346 | 350 |
| *A″ modes* | | | | |
| $\nu_{as}$ ($ClO_3$ stretch) | 1263 | ? | 1283 | inactive |
| $\delta_{as}$ ($ClO_3$ deformation) | 579 | 582 | 585 | inactive |
| $\rho$ (out-of-plane $ClO_3$ rocking) | 430 | 440 | 428 | inactive |
| $\tau$ ($ClO_3$ torsion) | 312 | 480 | 478 | inactive |

vibrational losses of molecular $HClO_4$ with increasing temperature. Most of the losses from the molecular layer disappear upon annealing to 173 K. Between 173 K and 213 K the spectra contain peaks at 460 $cm^{-1}$, 620 $cm^{-1}$, 885 $cm^{-1}$, 1115 $cm^{-1}$ and 1205 $cm^{-1}$. Finally, only three peaks at 620 $cm^{-1}$, 885 $cm^{-1}$ and 1205 $cm^{-1}$ remain after heating to 233 K. The observation of

Table 2
Assignment of fundamental vibrations of perchlorate ($ClO_4^-$, $T_d$ symmetry), infrared and Raman vibrational frequencies ($cm^{-1}$) [37]

| | | |
|---|---|---|
| $\nu_1$ ($A_1$) | $\nu_s$ (Cl–O stretch) | 932 |
| $\nu_2$ (E) | $\delta_s$ (Cl–O–Cl deformation) | 460 |
| $\nu_3$ ($F_2$) | $\nu_{as}$ (Cl–O stretch) | 1110 |
| $\nu_4$ ($F_2$) | $\delta_{as}$ (Cl–O–Cl deformation) | 626 |

Table 3
Assignment of fundamental vibrations of transition metal perchlorates [$Cu(ClO_4)_2 \cdot 2H_2O$, $C_{3v}$ symmetry, infrared and Raman vibrational frequencies ($cm^{-1}$)] [37] and adsorbed perchlorate on Au(111) (this work)

| | | $Cu(ClO_4)_2 \cdot 2H_2O$ | $ClO_4^{ads}$ |
|---|---|---|---|
| $\nu_1$ ($A_1$) | $\nu_s$ ($ClO_3$ stretch) | 1030 | 1205 |
| $\nu_2$ ($A_1$) | $\delta_s$ ($ClO_3$ bending) | 920 | 885 |
| $\nu_3$ ($A_1$) | $\nu_s$ (ClO* stretch) | 648 | 620 |
| $\nu_4$ (E) | $\nu_{as}$ ($ClO_3$ stretch) | 1158 | inactive |
| $\nu_5$ (E) | $\delta_{as}$ ($ClO_3$ stretch) | 620 | inactive |
| $\nu_6$ (E) | $\rho_r$ ($ClO_3$ rocking) | 480 | inactive |

Table 4
Assignment of fundamental vibrations of metal perchlorate complexes, [$Cu(ClO_4)_2$, $C_{2v}$ symmetry, infrared and Raman vibrational frequencies ($cm^{-1}$)] [37]

| | | |
|---|---|---|
| $\nu_1$ ($A_1$) | $\nu_s$ ($ClO_2$ stretch) | 1030 |
| $\nu_2$ ($A_1$) | $\nu_s$ (Cl–$O_2^*$ stretch)) | 948, 920 |
| $\nu_3$ ($A_1$) | $\delta_s$ ($ClO_2$ bending) | 665, 647 |
| $\nu_4$ ($A_1$) | $\delta_s$ ($ClO_2^*$ bending) | 466 |
| $\nu_5$ ($A_2$) | $\tau$ (torsion) | ? |
| $\nu_6$ ($B_1$) | $\nu_{as}$ (Cl–$O_2$ stretch) | 1130 |
| $\nu_7$ ($B_1$) | $\rho$ (rocking) | 624, 600 |
| $\nu_8$ ($B_2$) | $\nu_{as}$ (Cl–$O_2^*$ stretch) | 1270–1245 |
| $\nu_9$ ($B_2$) | $\rho$ (rocking) | 497 |

three vibrational losses under these conditions suggests the presence of a $ClO_4$ species with $C_{3v}$ symmetry which should exhibit three internal dipole active $A_1$ modes, according to Table 3 [37]. In addition one should observe the vibration of the whole $ClO_4$ complex against the surface, possibly at rather low frequency not resolved under the given experimental conditions, as mentioned above. While the losses at 620 $cm^{-1}$ and 885 $cm^{-1}$ are only slightly red shifted with respect to the corresponding values for the ClO* stretch vibration $\nu_s$ and the $ClO_3$ bending vibration $\delta_s$, the frequency of 1205 $cm^{-1}$ differs significantly from 1030 $cm^{-1}$ for the symmetric $ClO_3$ stretch vibration $\nu_s$ (compare Table 3). The strength of the symmetric $ClO_3$ stretch vibration $\nu_s$ is correlated with the Cl–O bond strength. As already pointed out by Stuve and co-workers, this mode depends on the coordination number [7]. $C_{3v}$ symmetry requires that the $ClO_4$ species are adsorbed either in a monodentate or tridentate configuration. The bonding to the Au(111) has to be performed by the oxygen lone-pair orbitals which are anti-bonding with respect to the Cl–O bond. Donation of charge into empty Au levels would strengthen the Cl–O bond, yielding an increased frequency of the symmetric $ClO_3$ stretch vibration $\nu_s$ [40]. Furthermore, such a high value of 1205 $cm^{-1}$ indicates a tridentate rather than a monodentate configuration [7,37].

In the temperature regime between 173 and 213 K a second perchlorate species can be detected with a lower $ClO_3$ stretch vibration $\nu_s$ of 1115 $cm^{-1}$. This shift to lower frequencies can be explained by a weaker interaction with the Au(111) surfaces caused by small amounts of coadsorbed $H_2O$, as proven and discussed in more detail below [7,40]. Consistently Sawatari et al. reported for a 0.1 M perchlorate solution on a Pt(111) electrode using IRAS that perchlorate ions adsorb in $C_{3v}$ symmetry in a monodentate or tridentate coordination at a positive potential range of 0.6–0.9 V vs. normal hydrogen electrode (NHE) [40]. Bands at $\sim$1119 $cm^{-1}$ and at $\sim$1230 $cm^{-1}$ were observed for the triply degenerate stretch $\nu_3$ stretch frequency of $ClO_4^-$ ions in solution or chemisorbed on the Pt(111) electrode, respectively.

### 3.3. Coadsorption of $HClO_4$ and $H_2O$ on Au(111)

To further investigate the influence of coadsorbed $H_2O$, we exposed a Au(111) surface precovered with different amounts of molecular $HClO_4$ to $H_2O$, as shown in Figs. 7 and 8. The subsequent adsorption of $H_2O$ results in a disappearance of the molecular $HClO_4$ loss features. Instead one observes in Fig. 7 for the larger $HClO_4$ precoverage similar losses as after annealing of molecularly adsorbed $HClO_4$ to 173 K (compare Fig. 6). It

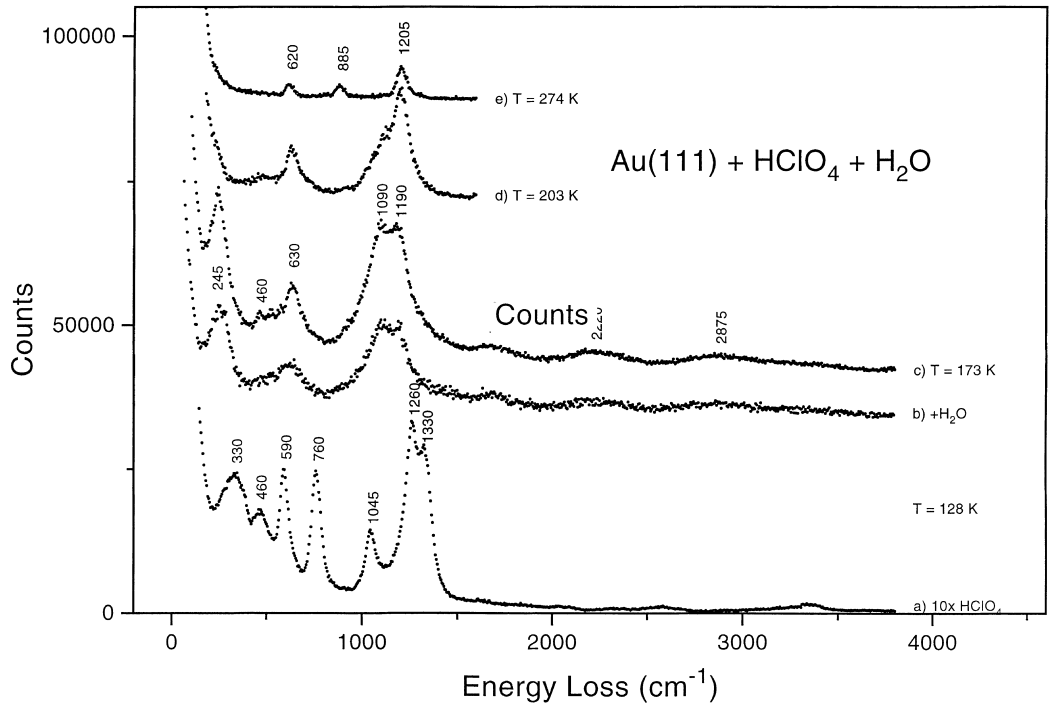


Fig. 7. HREEL spectra for coadsorbed $H_2O$ on Au(111) precovered with $HClO_4$ at 128 K and after a subsequent anneal to 173, 203 and 274 K for a large $HClO_4$ precoverage.

turned out that the intensity ratio of the $ClO_3$ stretch vibrations $\nu_s$ at 1090 $cm^{-1}$ and 1190 $cm^{-1}$ depends on the molecular ratio of coadsorbed $H_2O$ and $HClO_4$. The same amount of coadsorbed $H_2O$ added to a lower $HClO_4$ coverage (Fig. 8) results in a complete transformation of $HClO_4$ into "solvated" $ClO_4$ species with a single $ClO_3$ stretch vibration $\nu_s$ at 1145 $cm^{-1}$. Excess $H_2O$ can be detected by the appearance of the scissors mode at 1650 $cm^{-1}$ and a weak O–H stretch vibration at 3460 $cm^{-1}$. The frustrated librations of $H_2O$ are not resolved but lead to an increased broad background in the frequency range below 700 $cm^{-1}$. Hence the effect of coadsorbed $H_2O$ on molecularly adsorbed $HClO_4$ is two-fold. Obviously $H_2O$ induces the dissociation of molecularly adsorbed $HClO_4$ followed by a gradual solvation of the perchlorates species to an extent which depends on the stoichiometry between coadsorbed $H_2O$ and $ClO_4$ species.

A preferential desorption of hydration $H_2O$ from this layer can be achieved by a subsequent anneal. The resulting spectra resemble those obtained after heating a nearly anhydrous $HClO_4$ layer to elevated temperature, as discussed before in connection with Fig. 6. Only chemisorbed ("specifically adsorbed") $ClO_4$ species remain on the surface, which are stable up to at least 273 K. A decision as to whether solvated $ClO_4$ species desorb simultaneously with the hydration $H_2O$ or transform into directly adsorbed $ClO_4$ species cannot be made conclusively on the basis of HREELS intensities, which are not simply a quantitative measure for the corresponding concentrations.

The composition and chemistry of the coadsorbed $H_2O/HClO_4$ layer depends on the sequence of the exposure, as shown in Figs. 9 and 10. In the case of a small ($\Theta \approx 0.04$) $H_2O$ precoverage (Fig. 9) a subsequent $HClO_4$ exposure results in a HREEL spectrum exhibiting losses at 510 $cm^{-1}$, 640 $cm^{-1}$, 1115 $cm^{-1}$ and 1185 $cm^{-1}$ resembling the spectrum of Fig. 7b. Obviously $HClO_4$ does not adsorb molecularly in this case but dissocia-

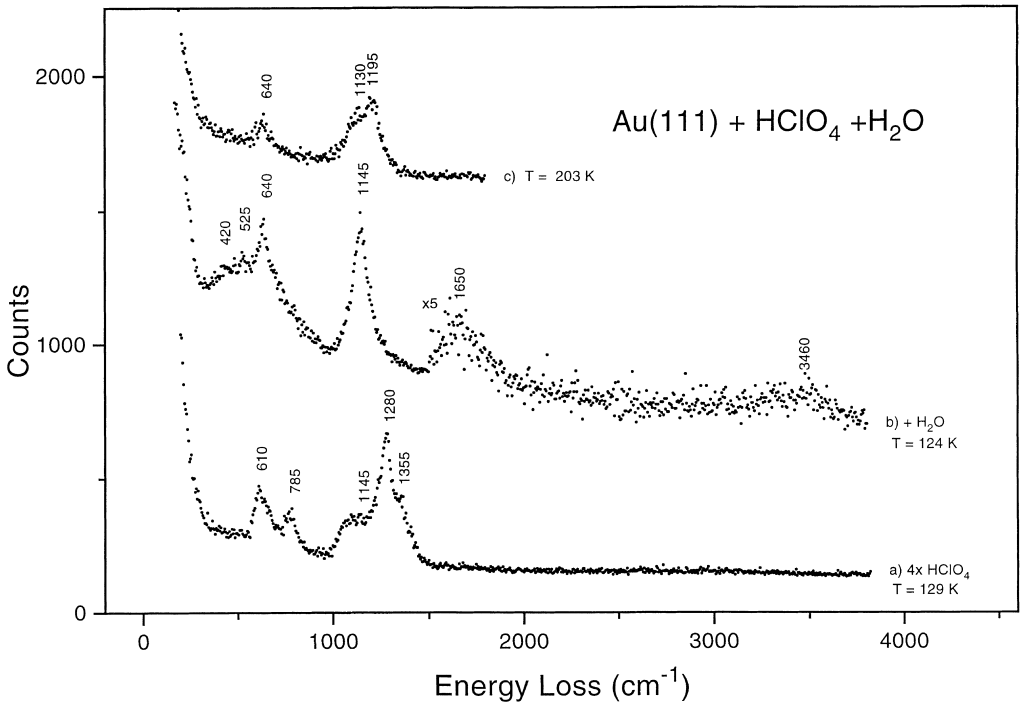


Fig. 8. HREEL spectra for coadsorbed $H_2O$ on Au(111) precovered with $HClO_4$ at 129 K and after a subsequent anneal to 203 K for a low $HClO_4$ precoverage.

tively. The dissociation products are perchlorate species partially solvated or directly adsorbed on the Au(111) surface, as evidenced by their corresponding $ClO_3$ stretch vibrations $\nu_s$ at 1115 $cm^{-1}$ and 1185 $cm^{-1}$, respectively. Upon increasing the $HClO_4$ exposure strong peaks appear at 620 $cm^{-1}$, 1050 $cm^{-1}$ and 1245 $cm^{-1}$. In addition less intense peaks at 2275 $cm^{-1}$, 2490 $cm^{-1}$ and broad bands around 2890 $cm^{-1}$ and 3075 $cm^{-1}$ can be discerned. This spectrum is different from that of molecular $HClO_4$ (Fig. 4) and cannot be explained by the perchlorate species discussed so far. An explanation for the observed vibrational losses can be given, assuming the formation of oxonium perchlorate ($H_3O^+ClO_4^-$). This compound is known as a solid protonic conductor and has been identified by various techniques, such as X-ray diffraction, IR, INS and Raman spectroscopy [41]. Particularly helpful for the elucidation of the vibrational modes shown in Fig. 9 are the Raman and INS frequencies. As a pyramidal molecule the $H_3O^+$ ion has four normal modes, which are listed in Table 5. By comparison the losses at 1050 $cm^{-1}$, 2890 $cm^{-1}$ and 3075 $cm^{-1}$ can be explained by the HOH bending mode $\delta_s$, the symmetric and asymmetric OH stretch frequency $\nu_s$ and $\nu_{as}$, respectively. The perchlorate ions, obviously not hydrated under these conditions, give rise to peaks at 620 $cm^{-1}$ and 1245 $cm^{-1}$. The remaining losses at 2275 $cm^{-1}$ and 2490 $cm^{-1}$ may be explained by combination losses or overtones, respectively.

From the annealing sequence in Fig. 9 it can be concluded that oxonium perchlorate is more stable than molecular $HClO_4$ and persists up to at least 193 K. Hence the desorption temperature is more than 40 K higher compared to molecularly adsorbed $HClO_4$. After the decomposition of these species upon annealing to higher temperature, partially solvated and directly adsorbed perchlorate species are left on the surface, as evidenced by their $ClO_3$ stretch vibrations at 1090 $cm^{-1}$ and 1190 $cm^{-1}$, respectively. The similarity of the spectra in the temperature range above 203 K

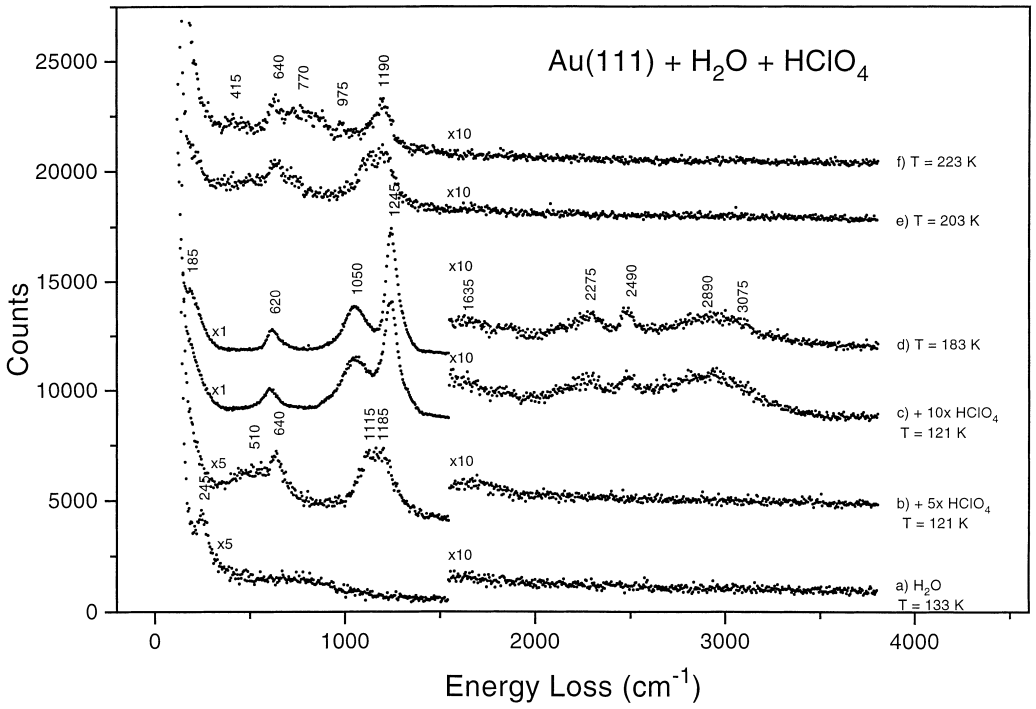


Fig. 9. HREEL spectra for coadsorbed $HClO_4$ on Au(111) precovered with $H_2O$ at 133 K for a low $H_2O$ precoverage and after a subsequent anneal to 183, 203 and 223 K.

suggests that the layer composition does not differ significantly from those obtained for molecularly adsorbed $HClO_4$ with or without $H_2O$ post-exposure.

Starting with a larger ($\Theta \approx 0.10$) $H_2O$ precoverage, more $HClO_4$ can be consumed by the dissociation, as shown in Fig. 10b. Heating to 163 K results in a completely changed loss structure with strong peaks at 640 $cm^{-1}$ with a broad tail to lower frequencies, at 1080 $cm^{-1}$ and 1185 $cm^{-1}$. Less intense features are seen at 1720 $cm^{-1}$ and 2360 $cm^{-1}$. The chemical composition of this layer is different from the lower $H_2O$ precoverage case in Fig. 9. Even after an anneal to 183 K some hydration water is left on the surface, as deduced from the broad librational structure below 640 $cm^{-1}$ and the bending mode at 1720 $cm^{-1}$. It can be concluded that the excess of preadsorbed water leads to the hydration of the oxonium perchlorate. Consistently the $ClO_3$ stretch frequency is slightly red shifted to 1185 $cm^{-1}$. This view is also supported by the observed OH stretch frequencies, unfortunately not amplified enough in the spectra of Fig. 10. But complementary data reveal losses in the OH stretch frequency range at 3390 $cm^{-1}$ and 3270 $cm^{-1}$ for hydration water and $H_3O^+$, respectively, shifted to higher values as expected with increasing solvation [42]. Again, the thermal stability of this solvated hydronium perchlorate ($nH_2O\ H_3O^+ClO_4^-$) seems to be higher than that of molecular $HClO_4$ in the nearly anhydrous state. An anneal to 183 K does not change the spectral features significantly until at 203 K losses appear similar to those for the reverse adsorption sequence as shown in Figs. 7 and 8.

The formation of oxonium perchlorate is supported by the observation of an ordered LEED pattern after annealing a coadsorbed layer with the right stoichiometry to 190 K. This LEED pattern could be identified as a $\begin{pmatrix} 3 & -1 \\ -1 & 2 \end{pmatrix}$ structure, also known as an oblique $(\sqrt{3} \times \sqrt{3})R30^\circ$ structure. Due to the extreme electron beam sensitivity of this structure, no screen shots can be presented. Instead schematic drawings of the LEED pattern

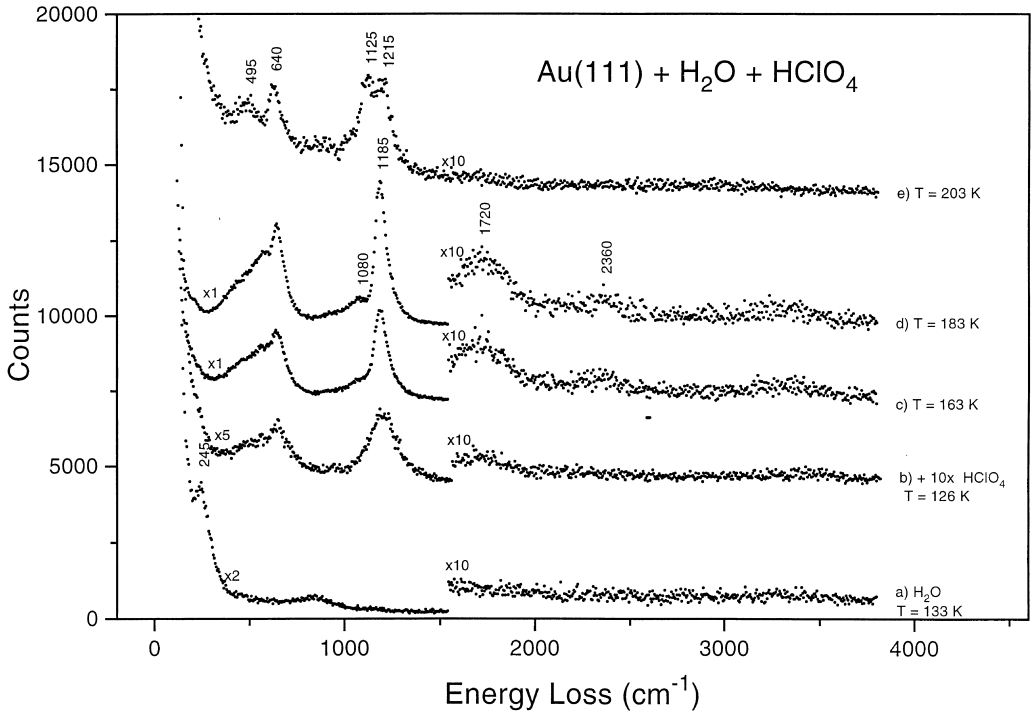


Fig. 10. HREEL spectra for coadsorbed $HClO_4$ on Au(111) precovered with $H_2O$ at 133 K for a large $H_2O$ precoverage and after a subsequent anneal to 163, 183 and 203 K.

Table 5
Assignment of $H_3O^+$ fundamental vibrations for oxonium perchlorate ($H_3O^+ClO_4^-$) in solution [infrared and Raman vibrational frequencies ($cm^{-1}$)] [41] and adsorbed on Au(111) (this work)]

| | | $H_3O^+ClO_4^-$ | $H_3O^+ClO_{4,ads}^-$ |
|---|---|---|---|
| $\nu_1$ ($A_1$) | $\nu_s$ (OH stretch) | 2890 | 2890 |
| $\nu_2$ ($A_1$) | $\delta_s$ (HOH bending) | 1043 | 1050 |
| $\nu_3$ (E) | $\nu_{as}$ (OH stretch) | 3160 | 3075 |
| $\nu_4$ ($E_1$) | $\delta_{as}$ (HOH bending) | 1649 | 1635 |

and the corresponding real space unit cell are shown in Fig. 5b. A similar pattern has been observed in "in situ" STM studies of bisulfate adsorption on Pt(111) after preparation under electrochemical conditions in sulfuric acid media by Stimming and co-workers [43]. The coverage and the stoichiometry of this mixed layer have been determined by XPS. Consistent with the oxonium perchlorate hypothesis, the $H_3O^+ClO_4^-$ ratio is near 1 with a molecular coverage of $\sim$0.2. This surface structure should be compared with the crystallographic structure of oxonium perchlorate (or perchloric acid monohydrate). Two crystal structures have been reported, namely a monoclinic and an orthorhombic with a phase transition at 252 K [41]. It is interesting to note that the low temperature monoclinic phase exhibits a layered structure which may favor the two-dimensional ordering for the UHV adsorption structure. Attempts to find under UHV conditions any analogues to the other well-known perchloric acid hydrate clathrate structure [44], which can be observed for a 5.5 $H_2O/ClO_4$ ratio, have failed so far.

## 4. Electrochemical relevance of adsorption studies in UHV

The link between "non situ" UHV model experiments and electrochemical studies is a common scale for the electrochemical potential and the

work function in vacuum [5,8]. Usually these two scales are aligned by the potential of the normal hydrogen electrode (NHE) corresponding to a work function of about $4.6 \pm 0.2$ eV [8]. In this context the work function of the Au(111) surface covered with a $H_2O/ClO_4$ layer, which exceeds the value of the clean surface of 5.3 eV by about 0.25 eV, should be compared with the situation at positive potentials in electrochemical cells. Consistently a positive potential of zero charge $E_{pzc} \approx 0.55$ eV vs. NHE has been observed in perchloric acid solution, also larger than 5 eV on the work function scale [45]. Under these conditions one expects that perchlorate can be specifically adsorbed, although it is generally considered to be an example for a non-specifically adsorbed, fully hydrated anion [21]. The appearance of directly adsorbed perchlorate $ClO_4$ has been shown by Sawatari et al. at a positive potential above 600 meV vs. NHE for a Pt(111) electrode [40]. Applying IR spectroscopy these authors found $ClO_3$ stretch frequencies at 1110–1119 $cm^{-1}$ and around 1200 $cm^{-1}$ for perchlorate ions in solution and perchlorate directly adsorbed on the electrode surface, respectively. Consistent with these findings we could identify chemisorbed perchlorate on Au(111) by a $ClO_3$ stretch frequency of about 1210 $cm^{-1}$. Accordingly Krasnopoler and Stuve showed that the tendency of adsorbed perchlorate being hydrated by coadsorbed $H_2O$ should decrease with increasing work functions of the substrates used [8]. They deduced from a Born–Haber cycle that the following condition has to be fulfilled in order to hydrate adsorbed perchlorate $ClO_4^{ads}$ by coadsorbing $H_2O$:

$$\Delta H_{ads} - \Phi_m \geq \Delta H_{hyd} - EA = -8.6 \text{ eV}. \quad (5)$$

This equation simply means that larger work functions of the $H_2O/ClO_4$/substrate surface, $\Phi_m$, and smaller heats of adsorption of neutral $ClO_4$ species, $\Delta H_{ads}$, make it more difficult for an adsorbed molecule to be ionized and hydrated, thereby gaining negative electron affinity, $EA$, and heat of hydration, $\Delta H_{hyd}$.

Therefore Krasnopoler and Stuve chose a Ag(110) single crystal surface with a comparably low work function of 4.2 eV, to demonstrate the transition from specifically to non-specifically adsorbed perchlorate under UHV. Upon $H_2O$ coadsorption the adsorbed perchlorate can be hydrated, as evidenced by the appearance of a $ClO_3$ stretch vibration at 1090 $cm^{-1}$. The difference in the heat of adsorption $\Delta H_{ads}$ of perchlorate on Ag(110) to Au(111) should not be significant. Since we observe an even weaker chemical interaction between $HClO_4$ and Au(111) compared to Ag(110), as indicated by a non-dissociative adsorption, $\Delta H_{ads}$ should be slightly smaller. For Ag(110) $\Delta H_{ads}$ has been estimated to be $-3.0$ eV with a contribution of only $-0.3$ eV from the heat of formation of $AgClO_4$. Hence the heat of adsorption for $ClO_4$ on Au(111) should lie between $-3.0$ and $-2.7$ eV. The larger work function for Au(111) and the weaker adsorption of $ClO_4$ on Au(111) make the left-hand side of the energy balance in Eq. (5) about 1 eV lower than for Ag(110), but still larger than the right-hand side. Thus chemisorbed perchlorate can be hydrated by coadsorbed $H_2O$, as shown by the occurrence of a $ClO_3$ stretch vibration at about 1145 $cm^{-1}$, also on a Au(111) surface, despite its relatively high work function of 5.3 eV.

Finally the tendency for H desorption should be increased for surfaces with a work function higher than the potential for hydrogen adsorption in an electrochemical cell. In the presence of coadsorbed $H_2O$ the unstable adsorbed H can induce the formation of oxonium ions ($H_3O^+$), as shown for $H_2O$ and H coadsorption on Pt(111) [46,47] and Pt(100) [48]. Interestingly enough this reaction does not occur on Cu(110) [49], which exhibits a smaller work function of 4.5 eV.

The influence of coadsorbed $H_2O$ on adsorbed $HClO_4$ on Au(111) is really two-fold. At first it induces $HClO_4$ dissociation into perchlorate chemisorbed or solvated. But under favorable conditions preadsorbed $H_2O$ reacts with the remaining H to oxonium $H_3O^+$, which could be identified by its corresponding vibrational modes. Oxonium perchlorate complexes adsorb in an ordered surface structure, similar to recent findings for bisulfate adsorption on Pt(111) electrodes under electrochemical conditions [43,50]. Furthermore, these adsorbed oxonium perchlorate species can be hydrated by excess $H_2O$, not consumed by the oxonium formation, to hydronium perchlorate.

## 5. Summary

In the present study it could be shown that model experiments under UHV conditions are well-suited to investigate the chemical interactions between electrolyte species at electrode surfaces. Especially vibrational spectroscopy using HREELS allows a straightforward identification of different adsorbed species. Molecular $HClO_4$ after adsorption on Au(111) surfaces at temperatures below 130 K can be clearly distinguished from perchlorate $ClO_4$, chemisorbed or solvated by coadsorbed $H_2O$. Coadsorbed $H_2O$ induces the dissociation of molecular $HClO_4$ into perchlorate either directly adsorbed or solvated by hydration water. Under favorable conditions oxonium perchlorate (or perchlorate monohydrate) ($H_3O^+HClO^-$) can be observed. By analogy the surface reactions under UHV conditions at the Au(111) substrate with a relatively high work function of 5.3 eV exceeding the corresponding value of a normal hydrogen electrode (NHE) can be compared with the situation in electrochemical cells at positive potentials.

## Acknowledgements

The continuous interest of Dr. W. Daum and his competent and valuable comments in numerous discussions contributed a great deal to this study. Stimulating discussions with E.M. Stuve and the critical reading of the manuscript by A. Wieckowsky are kindly acknowledged. The skilful and reliable technical assistance of Mrs. A.M. Franken during the course of the experiments is gratefully acknowledged.

## References

[1] J. Lipkowski, P.N. Ross (Eds.), Structure of Electrified Interfaces, VCH, New York, 1993.
[2] J.O'M. Bockris, A.K.N. Reddy, Modern Electrochemistry, Plenum Press, New York, 1970.
[3] A.T. Hubbard, Acc. Chem. Res. 13 (1980) 177.
[4] J.K. Sass, Vacuum 33 (1983) 791.
[5] D.M. Kolb, Zeits. für Phys. Chem. Neue Folge 154 (1987) 179.
[6] E.M. Stuve, N. Kizhakevariam, J. Vac. Sci. Technol. A 11 (1993) 2217.
[7] E.M. Stuve, A. Krasnopoler, D.E. Sauer, Surf. Sci. 335 (1995) 177.
[8] A. Krasnopoler, E.M. Stuve, J. Vac. Sci. Technol. A 13 (1995) 1681.
[9] J. Wang, B.M. Ocko, A.J. Davenport, H.S. Isaacs, Phys. Rev. B 46 (1992) 10321.
[10] M.J. Weaver, X. Gao, Ann. Rev. Phys. Chem. 44 (1993) 459.
[11] G. Luepke, G. Marowsky, R. Steinhoff, A. Friedrich, B. Pettinger, D.M. Kolb, Phys. Rev. B 41 (1990) 6913.
[12] P. Guyot-Sionnest, A. Tadjeddine, Chem. Phys. Lett. 172 (1990) 341.
[13] O.M. Magnussen, J. Hotlos, R.J. Nichols, D.M. Kolb, R.J. Behm, Phys. Rev. Lett. 64 (1990) 2929.
[14] S. Manne, P.K. Hansma, J. Massie, B.V. Elings, A.A. Gewirth, Science 251 (1991) 183.
[15] W.N. Hansen, C.L. Wang, T.W. Humpherys, J. Electroanal. Chem. 93 (1978) 87.
[16] D.M. Kolb, D.L. Rath, R. Wille, W.N. Hansen, Ber. Bunsenges. Phys. Chem. 87 (1983) 1108.
[17] F.P. Coenen, M. Kästner, G. Pirug, H.P. Bonzel, U. Stimming, J. Phys. Chem. 98 (1994) 7885.
[18] P. Baumann, G. Pirug, D. Reuter, H.P. Bonzel, Surf. Sci. 335 (1995) 186.
[19] G. Pirug, C. Ritke, H.P. Bonzel, Surf. Sci. 241 (1991) 289.
[20] D.M. Zehner, J.F. Wendelken in: R. Dobrozemsky, F. Rüdenauer, F.V. Viehböck, A. Breth (Eds.), Proc. 7th Int. Congr. and 3rd Int. Conf. on Solid Surfaces, Wien, 1977, p. 517.
[21] N. Kizhakevariam, R. Döhl-Oelze, E.M. Stuve, J. Phys. Chem. 94 (1990) 5934.
[22] Y.-E. Sung, S. Thomas, A. Wieckowsky, J. Phys. Chem. 99 (1995) 99.
[23] A. Wieckowsky, private communication.
[24] J.V. Barth, R. Schuster, R.J. Behm, G. Ertl, Surf. Sci. 348 (1996) 280.
[25] G. Pirug, unpublished results.
[26] J.H. Scofield, J. Electron Spectrosc. Relat. Phenom. 8 (1976) 129.
[27] A. van Eenbergen, E. Bruninx, J. Electron Spectrosc. Relat. Phenom. 33 (1984) 51.
[28] C.D. Wagner, L.E. Davis, W.M. Riggs, Surf. Interface Anal. 2 (1980) 53.
[29] P.W. Palmberg, G.E. Riach, R.E. Weber, N.C. MacDonald, Handbook of Auger Electron Spectroscopy, Physical Electronics Industries, 1972.
[30] B.D. Kay, K.R. Lykke, J.R. Creighton, S.J. Ward, J. Chem. Phys. 91 (1989) 5120.
[31] P.A. Thiel, T.E. Madey, Surf. Sci. Rep. 7 (1987) 211, and references cited therein.
[32] N.J. Tao, S.M. Lindsay, J. Appl. Phys. 70 (1991) 5141.
[33] M. Kiskinova, G. Pirug, H.P. Bonzel, Surf. Sci. 150 (1985) 319.
[34] G. Pirug, C. Ritke, H.P. Bonzel, Surf. Sci. 241 (1991) 289.

[35] H. Ibach, D. Mills, Electron Energy Loss Spectroscopy and Surface Vibrations, Academic Press, New York, 1982.
[36] A.I. Karelin, Z.I. Grigorovich, V.A. Rosolovskii, Spectrochim. Acta 31 (1975) 765.
[37] B.J. Hathaway, A.E. Underhill, J. Chem. Soc. London (1961) 3091.
[38] C.I. Ratcliffe, D.E. Irish, Can. J. Chem. 62 (1984) 1134.
[39] G.J. Valette, Electroanal. Chem. 122 (1981) 285.
[40] Y. Sawatari, J. Inukai, M. Ito, J. Electron Spectrosc. Relat. Phenom. 64/65 (1993) 515.
[41] M. Pham Thi, J.F. Herzog, M.H. Herzog-Cance, A. Potier, C. Poinsignon, J. Mol. Struct. 195 (1989) 293, and references cited therein.
[42] L.I. Yeh, M. Okumura, J.D. Myers, J.M. Price, Y.T. Lee, J. Chem. Phys. 91 (1989) 7319.
[43] A.M. Funtikov, U. Linke, U. Stimming, R. Vogel, Surf. Sci. L343 (1995) 324.
[44] D. Mootz, E.-J. Oellers, M. Wiebcke, J. Am. Chem. Soc. 109 (1987) 1200.
[45] U.W. Hammer, D. Dramer, R.S. Zhai, D.M. Kolb, J. Electroanal. Chem. 414 (1996) 85.
[46] F.T. Wagner, T.E. Moylan, Surf. Sci. 206 (1988) 187.
[47] D. Lackey, J. Schott, J.K. Sass, S.I. Woo, F.T. Wagner, Chem. Phys. Lett. 184 (1991) 277.
[48] N. Kizhakevariam, E.M. Stuve, Surf. Sci. 275 (1992) 223.
[49] D. Lackey, J. Schott, J.K. Sass, J. Electron. Spectrosc. Relat. Phenom. 54/55 (1990) 649.
[50] S. Thomas, Y.-E. Sung, H.S. Kim, A. Wieckowsky, J. Phys. Chem. 100 (1996) 11726.